JOURNAL OF SOLID STATE CHEMISTRY 14, 383–394 (1975)

Chemical Hysteresis in Phase Transitions in the Terbium Oxide–Oxygen System

A. T. LOWE AND L. EYRING*

Department of Chemistry, Arizona State University, Tempe, Arizona 85281

Received August 7, 1974; in revised form, November 19, 1974

A thermogravimetric study of hysteresis in the TbO_x–O_2 system has provided insight into phase transitions occurring among the fluorite-related rare earth oxides. A series of isobaric scanning loops at 380 Torr have been made. The scans were between $TbO_{1.5}(\varphi)$ and $TbO_{1.714}(\iota)$ at higher temperatures and between $TbO_{1.714}(\iota)$ and $TbO_{1.818}(\delta)$ at lower temperatures. Corresponding isobaric studies were made utilizing high temperature X-ray powder diffraction to augment the TGA experiments.

It was confirmed that sections of the lower temperature loop were dependent on the rate of temperature change while the higher temperature loop was entirely reproducible. Interior scanning loops made within the lower hysteresis loop showed univariant behavior typical of a single phase when reversed in the $\delta'\delta$ pseudophase region, otherwise it exhibited bivariant behavior. The upper hysteresis loop showed bivariant behavior throughout the interior of the loop. Some thermodynamic aspects and the microdomain concept as applied to hysteresis are also considered.

Introduction

Chemical hysteresis, the irreversible reaction cycle between two phases, despite its prevalence in many oxide systems is far from being well understood. Although there are a variety of causes of hysteresis unique to each case, the key to understanding lies in the details of the structural relationships of the end members of the phase reaction and in their intergrowth characteristics. One example where the causes are explained in these structural and textural terms is the TiO_x–O_2 system (*1*, *2*).

The structures of the rare earth oxides and their textural behavior in the two-phase regions are only now being clarified, opening the way to understanding their often observed hysteresis behavior. The present study has as its goal a detailed observation of hysteresis, including internal scanning loops and the occurrence of bivariant behavior termed *pseudophase* formation in the two-phase regions.

Hysteresis in these oxide systems is observed in terms of a difference in the temperature-composition isobaric path between heating and cooling. It is not an equilibrium phenomenon in the usual sense, which has led many to believe that hysteresis was caused by a slow phase reaction or sample impurity. However, metastable reproducible hysteresis is found in many solid state transitions of pure phases (this is also the case in adsorption hysteresis and magnetic hysteresis) (*3*). In this instance, the Gibbs free energy G, may be represented as

$$G = f(T, P, X, \sum \varphi)$$

where $\sum \varphi$ are all the factors other than temperature, pressure, and composition that might affect a phase transformation, e.g., a strain or surface term. Concomitantly the phase rule must be altered to add extra terms:

$$F = C - P + 2 + \sum \pi.$$

The TbO_x–O_2 system was chosen for this study because its large hysteresis loops are

* Author to whom inquiries should be sent.

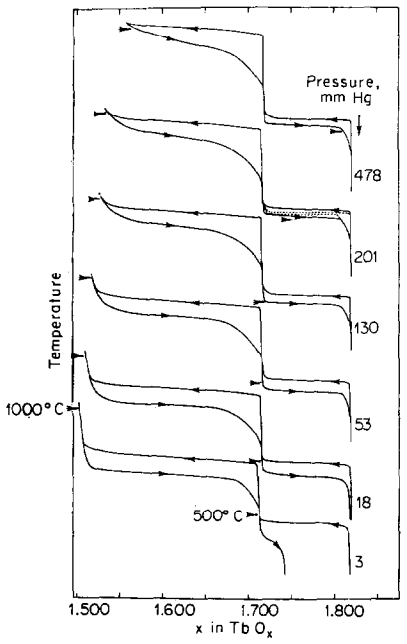

FIG. 1. Representative isobaric runs for the TbO_x–O_2 system.

between reasonably spaced intermediate phases at easily accessible temperatures and pressures (*4*, *5*). The isobars (*6*) of terbium oxide shown in Fig. 1 indicate three phases of narrow composition range at $TbO_{1.5+x}(\varphi)$, $TbO_{1.714}(\iota)$ and $TbO_{1.818}(\delta)$ as well as marked stability at $TbO_{1.809}(\delta')$. At the lowest pressures, diminished decomposition temperatures caused by hysteresis have resulted in a failure of ι to oxidize completely to δ. The change in slope of the cooling curve in each loop followed by marked bivariant behavior in the two-phase region is referred to as a pseudophase ($\sigma\iota$ or $\delta'\delta$).

Experimental Section

An 8 g sample of terbium oxide with a purity of 99.999% from the American Potash and Chemical Corporation was used for all experiments. These experiments were all made at 380 Torr oxygen. The thermogravimetric analysis was made on an Ainsworth RV-AU2 semimicrobalance system accurate to within ±30 μg described by previous investigators (*6*, *7*), but modified to include a pressure control device incorporating a Granville–Phillips leak valve and a capacitance manometer.

The semiautomated data acquisition system included a scanner, digital voltmeter, clock, and tape punch. The weight, temperature, and pressure read in millivolts were normally recorded on punched paper tape every 3 min on the first three channels of the scanner. The paper tape was converted to computer cards for data refinement on a CDC 6400 computer and for plotting on the CAL-COMP plotter.

The thermal correction was made by temperature cycling of a powdered Nd_2O_3 sample inert under the conditions of the experiment, having the same size as the TbO_x specimen. A least-squares fit was made to the weight variations of the blank and the TbO_x runs were corrected at each point. A correction for buoyancy was made from pressure-weight observations made at room temperature. The sum of these corrections was typically ±0.1 mg.

The X-ray studies were made with a high temperature Nonius–Guinier–Lenné camera, as described previously (*8*).

Results and Interpretations

Individual tensimetric experiments are summarized in Table I and plotted in Figs. 2–13. Each scan was necessary to explore some facet of the internal behavior of the particular hysteresis loop being studied.

The Effect of Heating Rate on the Hysteresis Loop

The rate of the phase reaction depends on the rate of oxygen diffusion and the rate of structural rearrangement to accommodate the composition change. From studies (*9*, *10*) of the diffusion of oxygen in the iota phase in the similar PrO_x–O_2 system it is safe to assume that at a heating and cooling rate of 0.5°C/min, oxygen is in equilibrium with the solid above 500°C. Although it is realized that due to lanthanide contraction the diffusion of oxygen in TbO_x would be somewhat slower than in PrO_x, the diffusion coefficients are sufficiently high at these temperatures to

warrant assumption of gas–solid equilibrium. The oxygen diffusion rate is unknown below 500°C and the structural transformation itself may be a rate-determining step at any temperature.

The effects of changing the heating and cooling rates between ι and δ are shown in Figs. 2 and 3. In each case the dashed curve represents a complete cycle between ι and δ at a rate of 0.5°C/min and will be referred to as the *primary curve*. It can be seen that the slower the heating and cooling rate, the smaller the hysteresis loop, except where previous investigators (*5–8*, *11*) have referred to pseudophase formation and the phase δ'.

The pseudophase region seems to be independent of the rate of traversal, therefore, oxygen is in equilibrium with the solid down

TABLE I

ISOBARIC SCANNING LOOPS OF THE TbO_x–O_2 SYSTEM (P_{O_2} = 380 TORR)

Figure number	Temperature ranges (°C)	Heating or cooling rate (°/min)	Phase composition sequences[a]
2	250 → 650 → 250	0.31	$\delta \rightarrow \iota + \delta \rightarrow \iota \rightarrow \iota + \delta' \rightarrow \delta' \rightarrow \delta + \delta' \rightarrow \delta$
3	250 → 650 → 250	0.059	$\delta \rightarrow \iota + \delta \rightarrow \iota \rightarrow \iota + \delta' \rightarrow \delta' \rightarrow \delta + \delta' \rightarrow \delta$
4	640 → 535 → 650	0.059	$\iota \rightarrow \iota + \delta' \rightarrow \delta' \rightarrow (\iota + \delta') \rightarrow \iota$
5	640 → 470 → 640	0.50	$\iota \rightarrow \iota + \delta' \rightarrow \delta' \rightarrow \delta' + \delta \rightarrow (\delta' + \delta) \rightarrow \iota$
6	740 → 510 → 530 → 200	0.50	$\iota \rightarrow \iota + \delta' \rightarrow \delta' \rightarrow \delta' + \delta \rightarrow (\delta' + \delta) \rightarrow \iota$
7	530 → 500 → 520 → 240	0.50	$\iota \rightarrow \iota + \delta' \rightarrow (\iota + \delta') \rightarrow \delta' \rightarrow \delta' + \delta \rightarrow \delta$
8	430 → 560 → 520 → 590 → 300	0.50	$\delta \rightarrow \delta + \iota \rightarrow (\delta + \delta' + \iota) \rightarrow \iota \rightarrow \delta' + \iota \rightarrow \delta' \rightarrow \delta' + \delta \rightarrow \delta$
9	290 → 530 → 230	0.50	$\delta \rightarrow \delta + \iota \rightarrow (\iota + \delta' + \delta) \rightarrow \delta' + \delta \rightarrow \delta$
10	1040 → 740 → 1040	0.50	$\varphi \rightarrow \sigma\iota \rightarrow (\sigma\iota) \rightarrow \varphi$
11, 12	1040 → 780 → 940 → 640	0.50	$\varphi \rightarrow \sigma\iota \rightarrow (\sigma\iota) \rightarrow (\sigma + \iota) \rightarrow \iota$
13	1040 → 880 → 1040 → 900 → 1040	0.50	$\varphi \rightarrow \varphi + \iota \rightarrow (\varphi + \iota) \rightarrow \varphi \rightarrow \varphi + \iota \rightarrow (\varphi + \iota) \rightarrow \varphi$
14	650 → 1000 → 650 → 983 → 650	0.50	$\iota \rightarrow \iota + \varphi \rightarrow (\sigma\iota + \iota) \rightarrow \iota \rightarrow \iota + \varphi \rightarrow (\sigma\iota + \iota) \rightarrow \iota$

[a] The parentheses indicate the internal section of the scanning loop sequence.

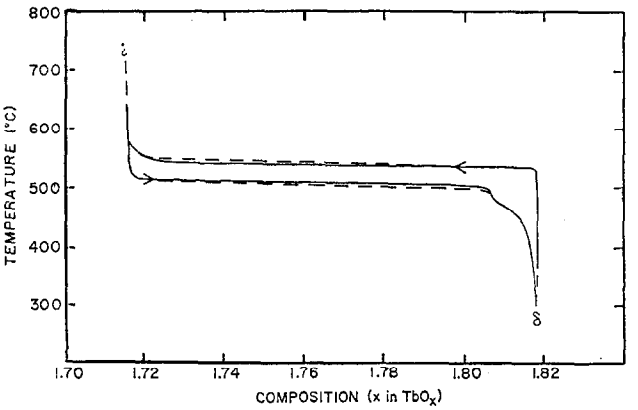

FIG. 2. Isobaric scanning loop between δ and ι of the TbO_x–O_2 system. Dashed line is 0.50°C/min and the solid line is 0.31°C/min.

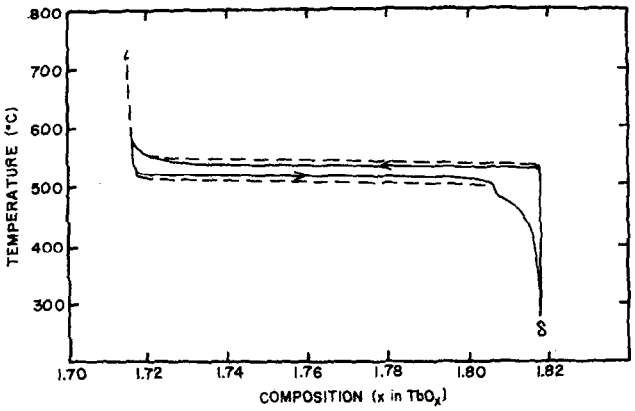

FIG. 3. Isobaric scanning loop between δ and ι of the TbO_x–O_2 system. Dashed line is 0.50°C/min and the solid line is 0.059°C/min.

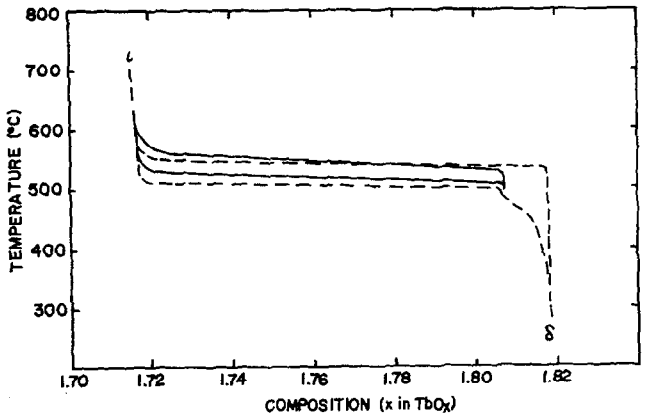

FIG. 4. Isobaric scanning loop between δ and ι of the TbO_x–O_2 system. Dashed line is the complete loop at 0.50°C/min between single phases and the solid line is the scanning curve at 0.059°C/min.

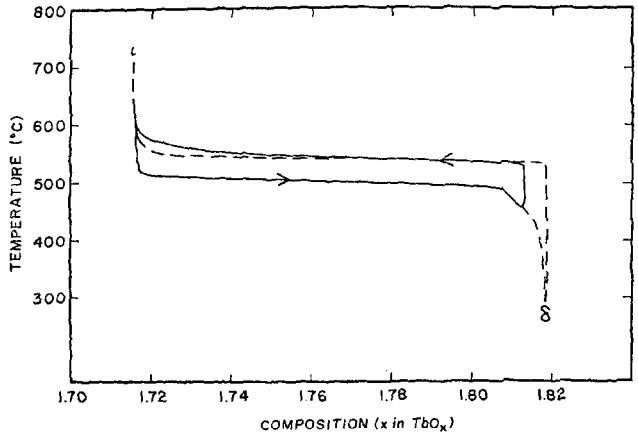

FIG. 5. Isobaric scanning loop between δ and ι of the TbO_x–O_2 system. Dashed line is the complete loop between single phases and the solid line is the scanning curve.

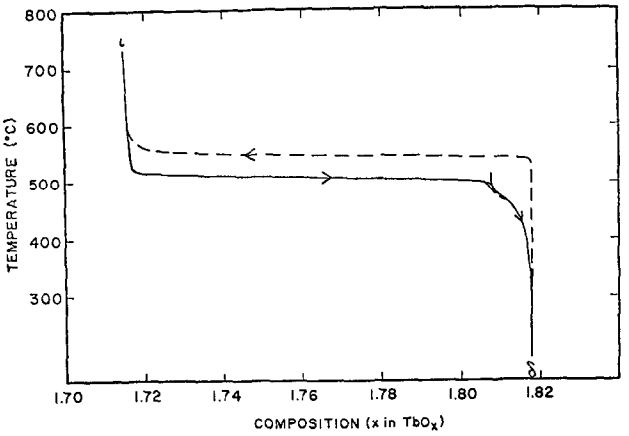

FIG. 6. Isobaric scanning loop between δ and ι of the TbO_x–O_2 system. Dashed line is the complete loop between single phases and the solid line is the scanning curve.

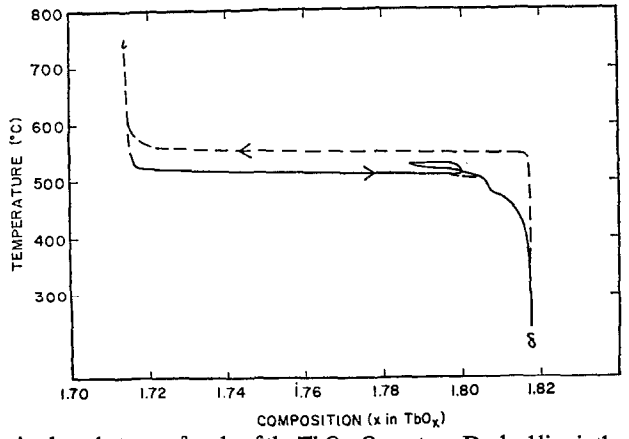

FIG. 7. Isobaric scanning loop between δ and ι of the TbO_x–O_2 system. Dashed line is the complete loop between single phases and the solid line is the scanning curve.

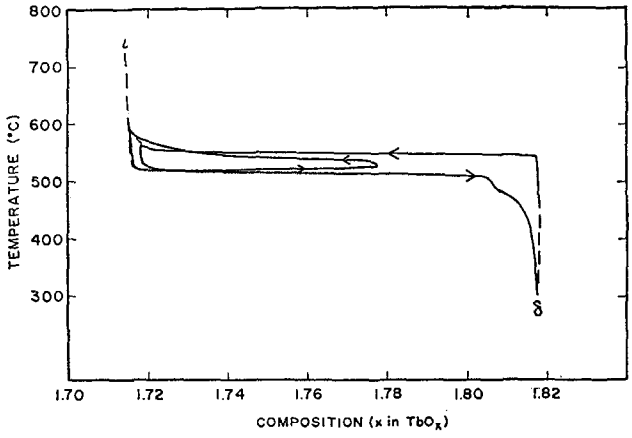

FIG. 8. Isobaric scanning loop between δ and ι of the TbO_x–O_2 system. Dashed line is the complete loop between single phases and the solid line is the scanning curve.

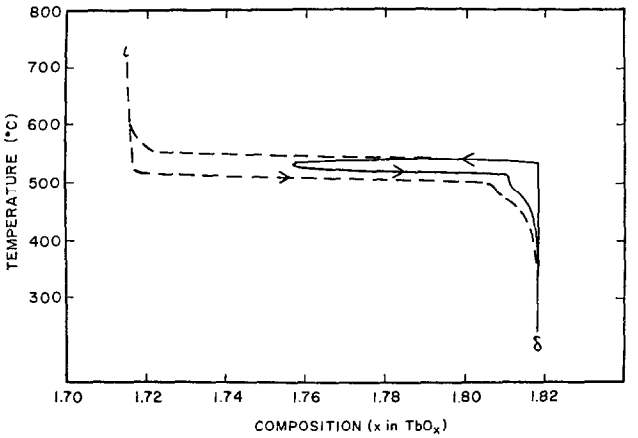

FIG. 9. Isobaric scanning loop between δ and ι of the TbO_x–O_2 system. Dashed line is the complete loop between single phases and the solid line is the scanning curve.

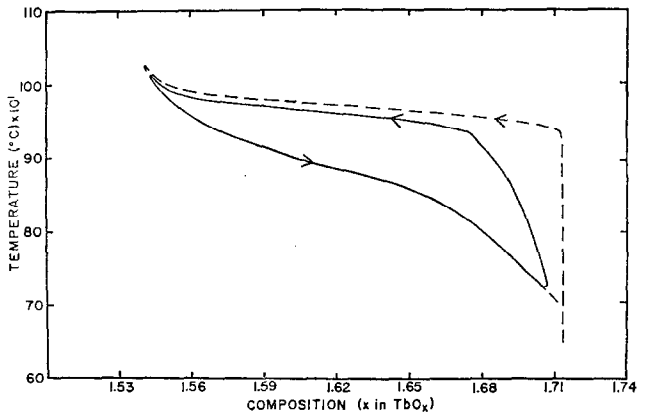

FIG. 10. Isobaric scanning loop between φ and ι of the TbO_x–O_2 system. Dashed line is the complete loop between single phases and the solid line is the scanning curve.

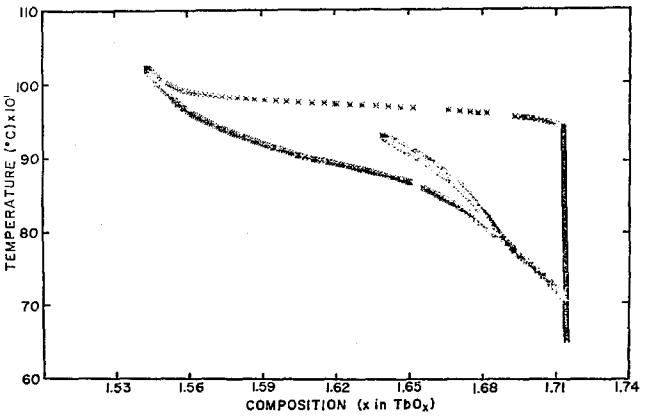

FIG. 11. Isobaric scanning loop between φ and ι of the TbO_x–O_2 system showing experimental points.

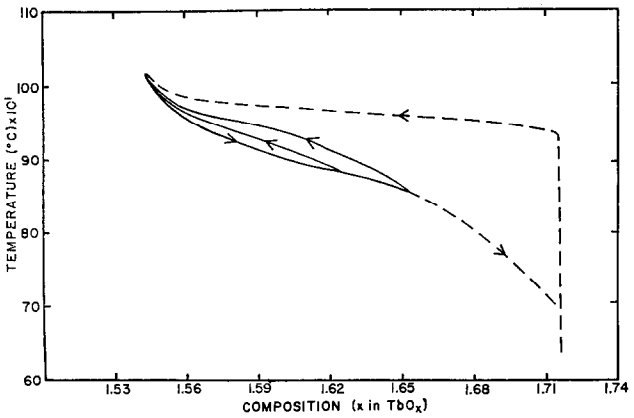

FIG. 12. Isobaric scanning loop between φ and ι of the TbO_x–O_2 system. Dashed line is the complete loop between single phases and the solid line is the scanning curve.

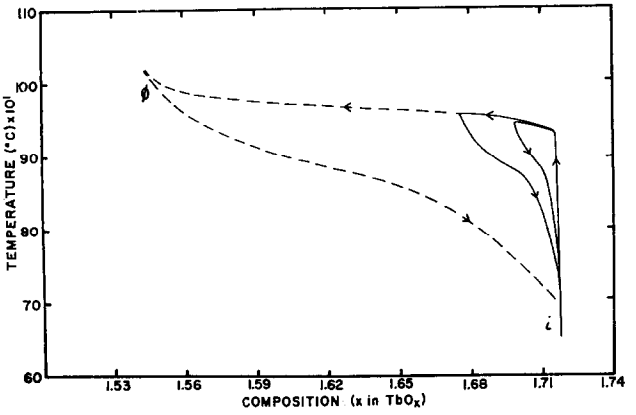

FIG. 13. Isobaric scanning loop between φ and ι of the TbO_x–O_2 system. Dashed line is the complete loop between single phases and the solid line is the scanning curve.

to a temperature of at least 350°C. This is consistent with previous powder runs made at these pressures (see Fig. 1). At lower pressures, however, the lower phase transformation temperature results in incomplete conversion of ι to δ below 300°C. It is clear that in this region under the conditions of these experiments the loop is time dependent outside the δ'–δ region but time independent in this region.

The high temperature X-ray diffraction observations revealed a distinct and separate phase $\delta'(TbO_{1.809})$. The lattice parameters of this phase were invariant at 450°C and 53 Torr over a period of 3 weeks. When the temperature was reduced from 450 to 300°C, over another 2 weeks the growth of δ at the expense of δ' was observed to be completed; however, the relative amount of each phase seemed to depend on only the temperature. These results are entirely consistent with the tensimetric observations. Table II demonstrates the satisfactory correspondence between these two types of observations.

In contrast similar experiments carried out between φ and ι at different heating and cooling rates showed no change in the size of the loop. The slowest heating rate was approximately 1°C/17 min where the loop could not be distinguished from that obtained at 0.5°C/min. The differences in the two loops

TABLE II

HIGH TEMPERATURE X-RAY ISOBARIC SCANNING LOOPS OF THE TbO_x–O_2 SYSTEM (P_{O_2} = 380 TORR)

Phase change	Temperature (°C)	Temperature from TGA experiments
$\iota \rightarrow \delta'$	522	519
$\delta' \rightarrow \delta$ (first appearance)	512	509
δ' (last appearance)	467	463
$\delta \rightarrow \iota$	537	537

are further emphasized with the internal scanning loops made on the balance.

X ray diffraction patterns were taken every 12 hr as the temperature was stepped at that frequency in 5–10° intervals between 870 and 590°C. The diffraction patterns confirmed the appearance of ι at 825°C growing at the expense of a σ phase (the symbol σ denotes a phase of variable composition related closely to φ) of decreasing lattice parameter until only ι was indicated at 770°C with no subsequent change except for thermal contraction down to 590°C. It was clear that the system was invariant during any 8-hr exposure made each 12-hr.

Scanning Loops between δ and ι

The first internal scan with the thermobalance is shown in Fig. 4. The sample was heated and cooled at the relatively slow rate of 1°C/17 min to identify the center of the δ' phase. The experiment was started with the specimen as ι phase, cooled, and then the temperature was reversed when the composition of δ' was reached. The δ' phase was heated until the ι composition was again obtained. The transition of δ' to ι occurs at a lower temperature than that of δ to ι. There are also marked differences in the two transition paths, e.g., the crossover, and hence, the higher temperature at which complete conversion to ι phase is achieved.

The scanning loop shown in Fig. 5 is similar to the one just described except that oxidation past δ' into the $\delta'\delta$ pseudophase is allowed before reversal and reduction to ι.

Upon reversing in $\delta'\delta$, the composition remains fixed until the top of the envelope is almost reached. This confirms that δ' phase as well as δ phase has essentially invariant composition up to its decomposition temperature and that interconversion of δ' and δ does not occur before decomposition of both to ι. A reversal at a composition that appears to be pure δ' followed by cooling before δ' decomposes is shown in Fig. 6. This reversibility is characteristic behavior of any of the single phases in this system.

A reversal in the two-phase region $\iota + \delta'$ (Fig. 7) shows the creation of an internal hysteresis loop. The reaction is interpreted as simply a conversion of δ' in the presence of ι, to ι followed by ι to δ'; there would be no δ involved.

The run illustrated in Fig. 8 is begun in δ then reversed just before ι is reached. A second reversal results in a path back to ι showing the crossover of the evelope typical of $\delta' \rightarrow \iota$ decomposition. This reversal in the $\iota \rightarrow \delta'$ path illustrates an important point. The V-shaped reversal is characteristic of a hysteresis loop that depends on the rate of temperature change. The reversal sequence must include slowing of the cooling rate, an arrest, and then an increase in the heating rate. This causes the loop to be squeezed toward whatever intrinsic core exists.

The experiment illustrated in Fig. 9 started in δ and was reversed in the $\iota + \delta$ region. This scan clearly illustrates the relationships between the three phases ι, δ, and δ'. At the reversal (V-shaped again but in the opposite sense from that shown in Fig. 8) there is approximately 60% ι and 40% δ, thereafter ι is being converted to δ' until the break point at which only δ' and δ remain in a 60–40 ratio. As the temperature is further reduced, δ' is being converted to δ. This scan suggests ι decomposes to δ' even in the presence of some δ and that δ' does not convert to δ except by pseudophase oxidation at lower temperatures.

Scanning Loops between φ and ι

For this series of scans the primary hysteresis loop is again marked with a dashed line and represents a cycle at 0.5°C/min between φ and ι. The primary loop that terminated at 1040°C does not show a reversible region of

single phase φ, hence it may possess a trace of ι when the oxidation path is begun. It was desirable to determine whether a sample containing no ι residue would exhibit the same oxidation features as one possibly containing a trace. In one run the oxygen pressure was reduced to vacuum at 1030°C until conversion to single phase φ was assured. The pressure was then restored to 380 Torr as φ oxidized in the single phase region to a value close to the normal primary loop and showed entirely parallel behavior in oxidation. Therefore, it is believed that no features of the arguments presented here are affected by the possibility of a trace of ι persisting when the oxidation was begun.

A high temperature X-ray diffraction isotherm at 1000°C confirmed the oxidation of φ in single phase (σ) but no ι was formed below 625 Torr, suggesting that ι is indeed absent in the experiment described above.

The scan shown in Fig. 10 was started in φ and reversed in the pseudophase region ($\sigma\iota$). There is no evidence that a unique phase of narrow composition occurs here, as in the case of δ' in the lower temperature loop, even though the break in the curve correlates somewhat with a composition Tb_6O_{10} ($TbO_{1.67}$), a member of the homologous series not yet observed in the TbO_x system. The high temperature X-ray studies reveal only $\sigma + \iota$ or ι alone in this region. In the reversed reaction the pseudophase character is retained until an approximate composition of $TbO_{1.67}$ is reached. As in the case for the $\delta'\delta$ region a characteristic hysteresis behavior defines the composition range of the $\sigma\iota$ region. However, the fact that the internal loop shows variable composition is in contrast to a reversal in $\delta'\delta$, where there is retention of composition until the edge of the primary curve is approached. Beyond the $\sigma\iota$ region there is a more pronounced two-phase behavior converting ι to φ.

A reversal in $\sigma\iota$ and then a second reversal in $\sigma\iota + \varphi$ is shown in Fig. 11. There is a slight internal loop shown by an unresolved broadening that closes when the $\sigma\iota$ region is reached.

For each of the isobaric loops shown in Figs. 2–13 the data points (usually between 1000 to 2000 points per run) are plotted and connected by a straight line. In Fig. 11, however, each point is represented by an asterisk to illustrate the closeness of successive readings.

The experiment depicted in Fig. 12 shows reversals in the two-phase region outside $\sigma\iota$. The small slope of the reduction branch of these loops should be contrasted with those initiated in the $\sigma\iota$ region (see Fig. 10). In this run and the next the absence of V-shaped curves characteristic of the slippage on reversal caused by the time dependence in the ι–δ region is clearly deomstrated (compare Figs. 8 and 9).

Two runs started in ι then reversed in $\iota + \varphi$ are shown in Fig. 13. The behavior here resembles that in the $\delta'\delta$ region in the sense that all the φ present converts to $\sigma\iota$, which then converts to ι by means of a pseudophase oxidation. For example, in the outer scan there is approximately 24% conversion of ι to φ and at the $\sigma\iota$ break in the oxidation curve there is about 24% $\sigma\iota$.

The high temperature X-ray diffraction of crystals of TbO_x in the two loops set some limits within which any discussion of hysteresis curves must stay. In the upper loop in reduction, ι is always seen to reduce to φ of virtually fixed lattice parameter; there is invariably a two-phase region in between. In oxidation, φ is seen to decrease in lattice parameter to varying degrees even before ι is formed and afterward they exist together to varying degrees of oxidation. The corresponding phase of variable composition in the PrO_x system has been called σ and in isotherms at about 800°C in the TbO_x–O_2 system it appears to have its maximum composition width, as indicated by the variation in lattice parameter.

The only phases appearing in the X-ray diffraction patterns in the upper loop are those to be expected from earlier quenched sample results except for the appearance of the σ phase of varying composition width. The occurrence of the pseudophase appears to be linked to the occurrence of σ, which yields phases of more compatible lattice parameters, enabling intergrowths of very good register. The diffraction pattern of the specimen in the pseudophase region is only that of ι phase.

Internal scanning loops indicated no diffraction effects except those expected from observations on the loop envelope and the tensimetric results.

High temperature diffraction from crystals in the lower loop confirms the earlier interpretation of the tensimetric results in that δ decomposes to ι with a two-phase region existing over a small temperature range. In oxidation ι decomposes first to $\delta'(TbO_{1.809})$ and then to δ with very limited variation in the diffraction patterns of any of the phases. The internal loops viewed by X-ray diffraction are entirely consistent with the observed tensimetric results including the failure of δ' to oxidize to δ unless the temperature is continually lowered, as indicated by the isobar. In addition, δ' is observed to convert directly to ι without formation of δ if the temperature is reversed and continually increased, as is clearly indicated in the scanning loops.

Discussion

The reproducibility of the $\delta' \rightarrow \delta$ section of the lower loop and of the entire higher temperature loop deomstrates intrinsic hysteresis in these systems that variation of ordinary experimental parameters does not eliminate. The effect of crystal size on intrinsic hysteresis is reported in a companion paper (*12*).

To be considered are the possible causes of hysteresis in these phase transformations. Such nonstoichiometric compounds may have the ability to retain a high degree of short-range order (*13*) and the two-phase region might consist of discrete domains of one composition and structure in a matrix of another. There is thought to be nearly perfect order within each domain, and the domains themselves, although oriented in relation to the matrix, are randomly dispersed. Associated with the boundary between these two phases will be an interfacial free energy. The form of this interfacial term is undetermined as yet, but it could result from an electrostatic lattice energy associated with having mismatched nearest neighbors or a volume strain energy due to the differences in dimension of the subcells of the two structures (*13*, *14*).

When considering the closely related structures of a homologous series it is reasonable to expect that they are coherently intergrown. In this case the size of the volume strain energy will depend on the difference in the *d*-spacings between the two phases and the acuteness of the angle at which they meet. Such domains have been seen in electron optical studies of the TiO_x–O_2 system (*2*) and are suggested from images taken of TbO_x crystals (*15*). It is believed that the difference in the interfacial free energy between the oxidation and the reduction paths is reflected in the intrinsic hysteresis between oxidation and reduction in the TbO_x–O_2 system. There would be a difference in the structural interface between domains of φ in ι versus domains of ι in φ. A further theoretical development of these ideas is presently underway.

The members of the homologous series Tb_nO_{2n-2} intergrow coherently. Nuclei of ι phase form in φ or σ and as they grow they must come together in a twinned orientation. It is probable that in the small crystallites of a powdered sample that a continuously twinned outer layer will encapsulate a core of partially oxidized but untransformed material or perhaps several cores within the same crystal. Of course when, for example, ι is reduced to φ, a related reverse process would occur. It is suggested that the difference in the surface free energy between nuclei of ι in φ and φ in ι cause hysteresis and that the final stages of reaction when the appearing phase isolates cores of the disappearing phase—pseudophase behavior results. This occurs in both directions, but it is much more pronounced when a phase with a larger molar volume is enclosed or when the crystal symmetry is lowered. It is also probable that the intergrowth capability is enhanced by the occurrence of σ phase in oxidation.

The high temperature X-ray results are consistent with this model since the material in the pseudophase region shows only the ι phase of fixed composition. The absence of diffraction from the cores could result from the strong absorption for X-rays reaching and

being diffracted from the interior as well as broadening of any emerging X-ray lines due to strain in the cores and/or their small size. Furthermore, the cores are likely to have a composition that moves the strongest diffraction lines very close to those of ι.

It is apparent from the temperature reversals made in the isobaric hysteresis loops that there are four types of behavior that elucidate the phase relationships in the system. In both loops temperature reversal in the reduction curve results in the immediate reoxidation of the newly formed phase, yielding a quantity of pseudophase proportional to the amount of reduced phase formed.

A second behavior type is also seen for both regions on reversal in the oxidation cycle. When reversal of the temperature occurs before the pseudophase region is reached, there is simple conversion to the more reduced phase.

To facilitate visualization of the other two types of hysteresis behavior on reversal in oxidation in the pseudophase regions themselves an analysis of the δ–ι loop is presented.

Three phases are occurring in this region, ι, δ, and δ', which give rise to two distinct loops, as illustrated in Fig. 4. The dashed line represents the experimental isobaric path $\iota \rightarrow \delta' \rightarrow \delta \rightarrow \iota$ when the temperature is cycled between 300 and 700°C and the solid line represents the $\iota \rightarrow \delta' \rightarrow \iota$ loop if the temperature is reversed immediately as δ' is reached. If instead, ι were to oxidize directly to δ the transformation would occur at a lower temperature than is experimentally observed.

The conversion of δ to δ' is not observed in any of the scanning experiments or high temperature X-ray studies. It is thought that δ' is a metastable phase with respect to δ, and hence, the $\delta \rightarrow \delta' \rightarrow \delta$ loop does not complicate the behavior further.

This could account for the differences between the reversals in the pseudophase $\varphi + \iota$ as opposed to $\delta + \delta'$. In the $\delta + \delta'$ region there is no conversion of δ to δ' and with an increase in temperature there is no further conversion to δ. The system then maintains composition until the transition temperature of δ' to ι is reached. In contrast, on reversing in the $\iota + \varphi$ pseudophase area there is immediate conversion of the ι regions of $\sigma\iota$ without forming *unlocked* φ at the φ interface. As soon as the φ structure is unlocked the slope changes to that characteristic of the $\iota \rightarrow \varphi$ transition. This defines the *region* boundaries of the pseudophase.

The δ' phase appears to be metastable with respect to δ at these temperatures. Electron diffraction studies (*16*) on the δ' phase, $TbO_{1.809}$, reveal a large triclinic unit cell that bears no apparent relationship to any other of the phases in the rare earth oxide homologous series Tb_nO_{2n-2}. Even its composition suggests a noninteger value of $n = 10\frac{1}{3}$, consistent with an observed multiplicity of 31 in the diffraction pattern compared to the parent fluorite structure.

It can be seen that the $\delta' + \delta$ two-phase region diverges from ideality much more than $\delta' + \iota$. If both of these two-phase systems are coherently intergrown, the behavior suggests that the strain term is larger for the $\delta' + \delta$ than for $\iota + \delta$. This means that the phases δ' and δ are more closely related and hence more tightly intergrown than are the phases ι and δ'.

It is also interesting to note that the two-phase regions that are the least ideal are the least temperature sensitive and hence are the most reproducible ($\sigma\iota$, $\delta'\delta$), while the regions that behave in a more classical manner ($\iota + \delta$, $\iota + \delta'$) are much more dependent on the heating and cooling rate. Intrinsic hysteresis then occurs when there is a high degree of intergrowth compatibility, and the greater this compatibility, the wider the loop.

A set of theorems was developed by Everett and his co-workers (*3*, *17*) to predict the behavior of internal scanning loops. The theorems applied to any type of hysteresis between any two states in which the scanning path is independent of scanning rate. This was thought to be applicable to the hysteresis in the rare earth oxides wherever the loop was not heating and cooling-rate dependent (as in the case between φ and ι in terbium oxide).

Everett's theorems were tested on the PrO_x–O_2 system by Faeth and Clifford (*18*) but unfortunately their scans were in a composition range where more than one two-phase area was crossed. With the scans made on the TbO_x–O_2 system, the set of rules

advanced by Everett were tested and found not to apply in most cases. The failure of Everett's theorems in this case are significant because they point to the possibility that there are more than two states (two structures) between φ and $\imath$. This is in accord with the reversals in $\imath + \varphi$ where the uniqueness of $\sigma\imath$ persists.

Acknowledgment

It is our pleasure to acknowledge the full support of the United States Atomic Energy Commission in the performance of these experiments.

References

1. L. A. Bursill and B. G. Hyde, "Progress in Solid State Chemistry" (H. Reiss and J. O. McCaldin, Eds.), Vol. 7, p. 177, Pergamon Press, Oxford (1972).
2. R. R. Marrett, B. G. Hyde, L. A. Bursill, and D. K. Philp, *Phil. Trans. Roy. Soc., Ser. A.* **274**, No. 1245, 627 (1973).
3. D. H. Everett and W. I. Whitton, *Trans. Faraday Soc.* **48**, 749 (1952).
4. E. D. Guth and L. Eyring, *J. Amer. Chem. Soc.* **76**, 5242 (1954).
5. B. G. Hyde and L. Eyring, "Rare Earth Research III" (L. Eyring, Ed.), p. 623, Gordon and Breach, New York (1965).
6. J. Kordis and L. Eyring, *J. Phys. Chem.* **72**, 2044 (1968).
7. M. S. Jenkins, R. P. Turcotte, and L. Eyring, "The Chemistry of Extended Defects in Non-Metallic Solids" (L. Eyring and M. O'Keeffe, Eds.), p. 36, North–Holland, Amsterdam (1970).
8. R. Turcotte, J. Warmkessel, R. Tilley, and L. Eyring, *J. Solid State Chem.* **3**, 265 (1971).
9. G. Weber and L. Eyring, "Advances in Chemical Physics" Wiley, New York (1971).
10. K. H. Lau, D. Fox, S. H. Lin, and L. Eyring, to be published.
11. B. G. Hyde, D. J. Bevan, and L. Eyring, *Phil. Trans. Roy. Soc. London, Ser. A.* **259**, No. 1106, 583 (1966).
12. A. T. Lowe, K. H. Lau, and L. Eyring, *J. Solid State Chem.* to appear.
13. J. S. Anderson, "Problems of Nonstoichiometry" (A. Rabenau, Ed.), p. 1, North–Holland, Amsterdam (1970).
14. A. R. Ubbelohde, *Proc. Roy. Soc., London, Ser. A.* **159**, 301 (1937); *Quarterly Rev. Chem. Soc., London* **11**, 246 (1957).
15. E. Summerville and L. Eyring, unpublished data.
16. P. Kunzmann and L. Eyring, in press.
17. D. H. Everett and F. W. Smith, *Trans. Faraday Soc.* **50**, 187 (1954); D. H. Everett, *Trans. Faraday Soc.* **50**, 1077 (1954); D. H. Everett, *Trans. Faraday Soc.* **51**, 1551 (1955).
18. P. A. Faeth and A. F. Clifford, *J. Phys. Chem.* **67**, 1453 (1963).